applied sciences

MDPI

Article

Experimental Study on Rock Strength Parameters of Ultra-Deep Carbonate Reservoirs Under Multiple Working Conditions with Scratch Test

Zhendong Liu [1,2,3], Xinpu Shen [4,5,*], Wenhai Ma [1,2,3], Yicheng Song [5], Guoqiang Shu [1,2,3] and Jinxin Liu [1,2,3]

[1] Daqing Oilfield Production Technology Institute, Daqing 163453, China; liuzhendong@petrochina.com.cn (Z.L.); mawenhai@petrochina.com.cn (W.M.); shuguoqiang@petrochina.com.cn (G.S.); liujinxin1995@petrochina.com.cn (J.L.)
[2] Heilongjiang Provincial Key Laboratory of Oil and Gas Reservoir Stimulation, Daqing 163453, China
[3] State Key Laboratory of Continental Shale Oil, Daqing 163453, China
[4] College of Petroleum Engineering, China University of Petroleum, Beijing 102249, China
[5] College of Oil and Gas Engineering, Liaoning Petrochemical University, Fushun 113001, China; songyicheng@stu.lnpu.edu.cn
* Correspondence: shen2022@cup.edu.cn

Abstract

Accurate determination of rock mechanical parameters for ultra-deep carbonate reservoirs (>9000 m) is critical for wellbore stability evaluation and acid-fracturing parameter optimization, yet systematic experimental data for such depths remain scarce. This study investigates grainstone cores from the YS Section (9199.8–9624.0 m) of Well XY in the Tarim Basin using continuous scratch tests—a minimally destructive method providing continuous strength profiles—complemented by conventional uniaxial compression tests. Five working conditions are systematically compared: original (unsoaked) state, drilling-fluid instantaneous contact (0 h), fresh water immersion (24 h), drilling-fluid immersion (24 h), and 15% hydrochloric-acid immersion (24 h). In the original state, scratch-test averages yield a uniaxial compressive strength (UCS) of 179.9 MPa, internal friction angle of 34.2°, and cohesion of 47.6 MPa. None of the three water-based working fluids causes measurable strength degradation within 24 h, with UCS values of 191.6, 186.0, and 190.9 MPa, respectively, attributable to the low water sensitivity of carbonate minerals. In contrast, 24 h acid immersion reduces UCS to 109.2 MPa (−39.3%), cohesion to 29.0 MPa (−39.0%), and internal friction angle to 27.1° (−20.6%), driven by intergranular cement dissolution, with strong sample-dependent variability (individual UCS reductions ranging from 12.6% to 48.0%). Scratch depth significantly influences results: UCS at 0.20 mm depth is 30.3% lower than at 0.18 mm. Calibration against rigid-testing-machine UCS yields a ratio coefficient $\alpha = 0.47\sim0.61$. A value of 0.56 is set for α, giving a recommended engineering UCS of 100.7 MPa. These findings provide an experimental basis for wellbore stability analysis and acid-fracturing design in ultra-deep carbonate reservoirs.

Keywords: carbonate rock; continuous scratch test; rock mechanical parameters; acid immersion; drilling fluid

Check for updates

Academic Editor: Andrea Carpinteri

Received: 13 September 2026
Revised: 25 October 2026
Accepted: 29 October 2026
Published: 31 October 2026

Copyright: © 2026 by the authors. Licensee MDPI, Basel, Switzerland. This article is an open access article distributed under the terms and conditions of the Creative Commons Attribution (CC BY) license.

1. Introduction

Deep and ultra-deep carbonate rocks have become an important replacement domain for oil and gas reserve growth and production increase in China. The main producing intervals in basins such as the Tarim and Sichuan basins are generally buried deeper than 7000 m,

and some intervals have reached depths beyond 9000 m [1]. With increasing burial depth, the formation pressure system becomes complex, the in situ stress differential increases, and reservoir heterogeneity intensifies, leading to a significant increase in complex conditions such as wellbore instability, collapse, and pipe sticking. The core inputs for wellbore stability evaluation and collapse-pressure calculation are rock strength parameters (uniaxial compressive strength, internal friction angle, and cohesion) and elastic parameters, whose values directly determine the design outcome of the safe mud-weight window [1]. Among them, the uniaxial compressive strength (UCS) is a commonly used rock strength parameter with a long research history and extensive literature [1–5]. The conventional method for measuring UCS is to use a rigid uniaxial compression testing machine; the experimental process is relatively complex and costly. Therefore, seeking a simpler, low-cost, portable, and fast-operating rock strength testing method has become an engineering necessity.

The scratch test is a new method for measuring rock strength parameters [6,7]. The DD model proposed in Reference [6] decomposes the total force acting on the cutting tooth into a cutting-face force and a wear-plane friction force, assuming the two are uncoupled, thereby introducing three basic parameters: intrinsic specific energy ε (which can be regarded as a measure of UCS), the vertical/horizontal cutting force ratio ζ, and the rock–tooth interface friction coefficient μ. This model is the theoretical basis for all subsequent cutting-test methods for determining rock strength. Reference [7] systematically elaborated the method for determining rock strength parameters using cutting tests. Based on the DD model, they performed scratch tests on cores using self-developed experimental equipment, proving that $\mu = \tan\varphi = Fn/Fs$ can be regarded as the internal friction angle of the rock, where Fn is the normal force and Fs is the shear force applied on the cutting tool, while ε can serve as a direct measure of UCS. This method has the advantages of low cost, portability, fast operation, and relatively non-destructive continuous testing of cores, laying the foundation for subsequent commercial rock strength testers. Reference [8] discussed the influence of parameters such as cutting depth on the experimental results of intrinsic specific energy ε and further applied scratch tests to sedimentary rock strength determination, establishing a quantitative dependence between cutting force and rock mechanical parameters and promoting the technology from the laboratory to the oilfield site. Reference [9] comprehensively demonstrated the advantages of scratch tests in determining the strength and elastic parameters of sedimentary rocks: higher resolution and data density than logging curves, continuous measurement compared with conventional core tests, and applicability to engineering problems such as reservoir compaction, hydraulic fracturing, wellbore stability, and sand production. Reference [10] compared the correlation between intrinsic specific energy ε and UCS through extensive experiments, proving that the two are positively correlated; under the same experimental conditions, data from quarry limestone showed that the maximum error between the two does not exceed 20%, data from quarry sandstone showed a maximum error of 23.3%, and data from low-strength shale showed an error of 50%, where the intrinsic specific energy was greater than the UCS value. The results of Reference [10] indicate that the strength calibration factor α between the intrinsic specific energy obtained from scratch tests and UCS is generally close to 1 but varies with lithology. When using relevant experimental results, the value of the strength calibration factor α should first be calibrated before good results can be obtained.

Reference [11] studied the determination of rock strength parameters in complex formations using the continuous scratch method, establishing a set of continuous scratch test parameter-setting methods and experimental procedures that address issues such as scratch-sequence interference, scratch-position substitution, and differences in rock-breaking modes at different scratch depths. Reference [12] studied continuous dynamic core-scratching test technology and proposed a continuous dynamic core-scratching test

technique. Reference [13] studied the classification criterion for coal burst propensity based on scratch testing, establishing a classification criterion based on scratch specific energy.

Carbonate rocks belong to sedimentary rocks and are mainly composed of carbonate minerals such as calcite ($CaCO_3$) and dolomite ($CaMg(CO_3)_2$), with common types including limestone and dolomite. During drilling, completion, and reservoir stimulation, wellbore rocks inevitably come into contact with working fluids such as drilling-fluid filtrate, formation water, and acid. Existing studies have shown that acid dissolution reactions with carbonate rocks significantly degrade the mechanical integrity and stiffness of the rock and transform its mechanical behavior from brittle to ductile [14,15], whereas the effect of water-based working fluids on carbonate rocks is relatively complex, with the degree of influence closely related to rock mineral composition, cementation type, and action time.

At present, systematic comparative studies targeting ultra-deep carbonate rocks deeper than 9000 m and incorporating drilling fluid, fresh water, and acid into a unified experimental system are still relatively scarce. The evolution direction and magnitude of strength parameters under different fluid actions remain unclear, and engineering design often generically treats them as "immersion implies reduction," lacking experimental basis. In this paper, taking ultra-deep grainstone cores from the YS Section of Well XY as the object, scratch-mechanical comparative experiments under five working conditions are carried out, and, combined with conventional rigid-testing-machine uniaxial compression strength tests, the rock strength parameter values under each working condition are quantitatively given, providing directly citable experimental evidence for ultra-deep carbonate wellbore stability analysis and acid-fracturing stimulation design.

2. Materials and Experimental Methods

2.1. Sample Characteristics and Sampling

The experimental cores were taken from the YS Section of Well XY in the Tarim Basin, comprising two intervals: 9199.8–9204.3 m and 9619.36–9624.0 m, with a lithology of grainstone. The sample specification is 2.5 cm in diameter × 5 cm in length. The sampling plan is given in Table 1. The samples were prepared by drilling, cutting, grinding, and cleaning, and excessive disturbance of the native structure of the rock samples was avoided during preparation. In the sample numbering, the first digit N1 indicates the interval from which the core was taken, the second digit N2 indicates the N2-th coring, and the third digit N3 indicates the N3-th core in that coring. For example, core 1-1-1 denotes the first core of the first coring in the first interval (9199.8–9204.3 m).

Table 1. Sampling plan.

Interval No.	Well No.	Stratum	Depth/m	Lithology	No. of Samples	Specification	Analysis Item
1	Well XY	YS Section	9199.8–9204.3	Grainstone	10	2.5 cm × 5 cm	Continuous scratch strength test
2	Well XY	YS Section	9619.36–9624.0	Grainstone	10	2.5 cm × 5 cm	Continuous scratch strength test

2.2. Experimental Instruments

The main instruments include a rock scratch tester, a microcomputer-controlled electro-hydraulic servo uniaxial compression testing machine, an LVDT displacement acquisition system, an electronic balance, a high-precision vernier caliper, and auxiliary equipment for

core drilling, cutting, grinding, and cleaning. The continuous core scratching test apparatus along with afore mentioned apparatus were manufactured by the Institute of Rock and Soil Mechanics, Chinese Academy of Sciences. All instruments have passed calibration. The scratch tester consists of a frame, a moving carriage, a vertical positioning and loading system, a high-precision force sensor, a diamond cutter, and a data acquisition system; its structure is shown in Figure 1a. During the scratch test, the cutter moves horizontally at a constant rate, the normal and tangential forces are synchronously recorded at a high sampling frequency, and the displacement is independently acquired by the LVDT, ensuring the resolution of the force–displacement curve.

The angle of the cutting edge at the cutter head is 87°, the cutter body width is 5 mm, the rake angle is 15°, and the scratch depth is d, as shown in Figure 1b.

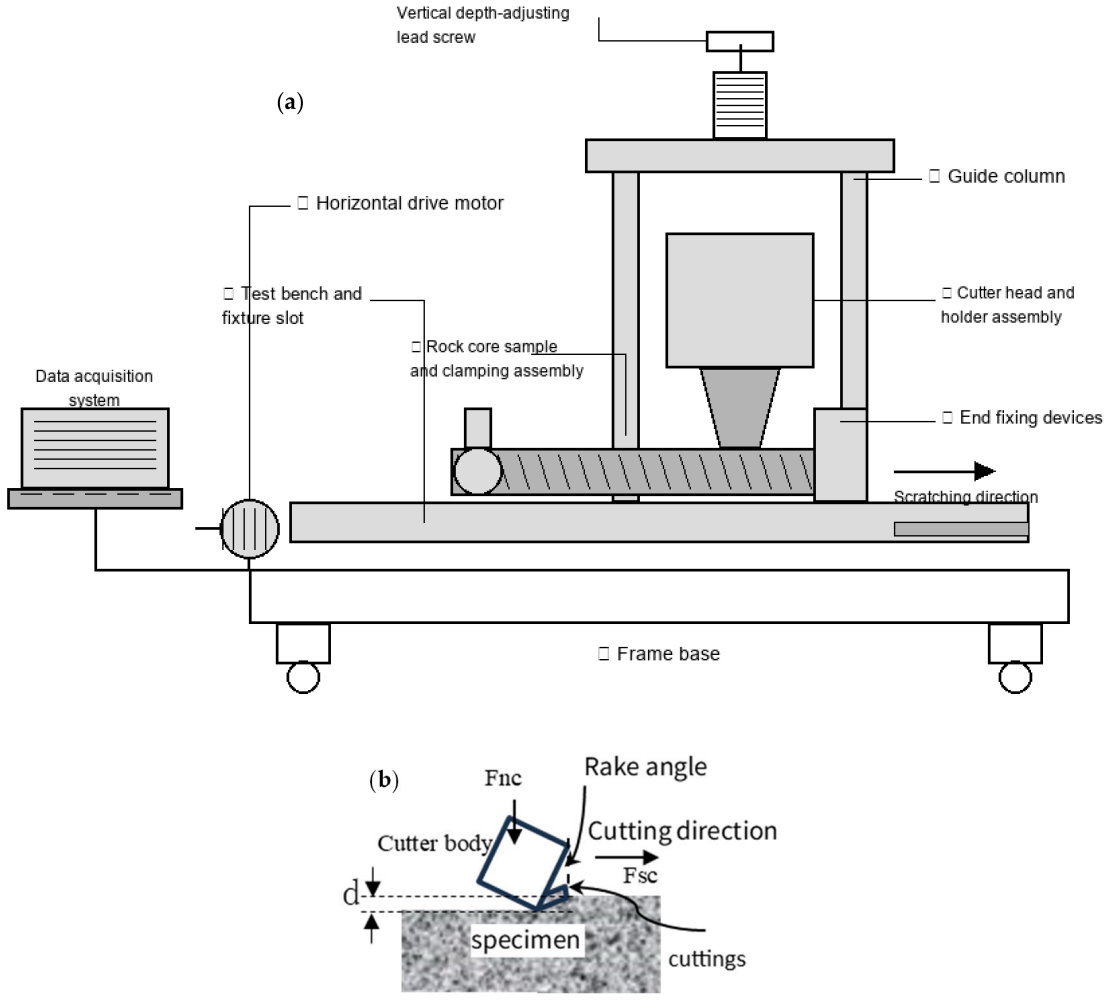


Figure 1. Schematic diagram of the rock scratch tester structure. (**a**) Overall structure of the scratch tester; (**b**) cutter geometry and force definitions.

2.3. Experimental Media

The experimental media were all taken from actual field engineering fluids, including commonly used field KCl-polysulfonate drilling fluid, formation-water simulant (fresh water), and acid (15% hydrochloric acid). The field carbonate reservoir stimulation (acid fracturing) process is relatively complex: generally, acid-free pad fluid is first pumped to create hydraulic fractures, then acid is pumped with corrosion inhibitor added to reduce corrosion of tubing and equipment and alternately injected with other working fluids to expand the acid sweep range. Among them, the core medium that plays a key role in rock

mechanical properties is the acid. To simplify the process and shorten the experimental cycle, the acid condition in this paper only adopts constant-temperature acid immersion for 24 h at room temperature and atmospheric pressure in a 5-gallon barrel, without expanding the complete acid-fracturing multi-fluid system. In field application, it is necessary to combine the experimental acid concentration with the effective acid content in the actual stimulation fluid and consider the coupling effect of contact time for comprehensive evaluation.

2.4. Working-Condition Settings

A total of five working conditions were set in the experiment: ① Untreated room-temperature condition (unsoaked); ② KCl-polysulfonate drilling fluid 0 h instantaneous contact; ③ fresh water 24 h immersion; ④ KCl-polysulfonate drilling fluid 24 h immersion; ⑤ acid 24 h immersion. The temperature of all five conditions was conventional room temperature. Scratch tests in each group uniformly adopted a standard scratch depth of 0.25 mm; some comparison groups additionally set gradient depths of 0.18 mm and 0.20 mm to investigate the influence of cutting depth. Two parallel scratches were performed on each core sample, and multiple parallel core samples were used for each condition group to minimize experimental errors caused by heterogeneity. The working-condition settings are given in Table 2.

Table 2. Experimental working-condition settings.

Working Condition	Medium	Action Time/h	Scratch Depth/mm	Sample Numbers	Parallel Scratches
As-received (unsoaked) condition	—	0	0.25	1-4-3, 2-7-1, 2-7-3, 2-8-1, 2-8-2	2
Drilling fluid 0 h instantaneous contact	Field drilling fluid	0 (instantaneous wetting)	0.25	1-4-1, 1-4-2, 2-4-1, 2-5-1, 2-5-2	2
Fresh water 24 h immersion	Fresh water (formation-water simulant)	24	0.25	1-4-3, 2-7-1, 2-7-3, 2-8-1, 2-8-2	2
Drilling fluid 24 h immersion	Field drilling fluid	24	0.25	1-4-1, 1-4-2, 2-4-1, 2-5-1, 2-5-2	2
Acid 24 h immersion	15% hydrochloric acid	24	0.18–0.25	1-1-1, 1-2-1, 2-1-2, 2-3-1, 2-3-2	2

2.5. Experimental Reference Standards

The uniaxial compressive strength test was carried out in accordance with SY/T 5367—2019 "Test Method for Uniaxial Compressive Strength of Rock" [16], and the scratch mechanical property test was carried out in accordance with generally accepted industry specifications.

2.6. Continuous Scratch Test Principle and Data Processing

The continuous scratch test uses a sharp diamond cutter of known width to scribe a groove on the sample surface at a constant shallow cutting depth ($d < 1$ mm) and constant horizontal rate, while synchronously acquiring the normal and tangential forces acting on the cutter as well as the horizontal displacement. Studies have shown that rock cutting exhibits two failure modes, ductile and brittle, whose transition is controlled by cutting depth: under shallow cutting depth, the ductile mode dominates, and the force on the cutting face is proportional to the groove cross-sectional area, with the proportionality coefficient defined as the rock intrinsic specific energy ε. The intrinsic specific energy is

obtained by force–displacement integration, and, combined with Coulomb strength theory, the uniaxial compressive strength, internal friction angle, and cohesion of the rock can be continuously inverted along the scratch direction to obtain the strength parameter values of the sample. Here, the cohesion CS is calculated from the experimental results of UCS and internal friction angle φ according to Equation (1):

$$CS = (UCS\ (1 - \sin \varphi))/(2\cos \varphi) \quad (1)$$

Data processing adopted a unified approach: after removing approximately 10% from both the beginning and end of the measurement-point sequence of each scratch, the arithmetic mean of the middle segment was taken as the mechanical parameter of that scratch; sample-level results were obtained by weighting the two parallel scratches of that sample by the number of effective points; the overall value of a working condition was obtained by reweighting all samples of that condition by the number of effective points. The number of effective data points for each condition ranged from 4238 to 4624, providing sufficient sample size.

2.7. Uniaxial Compression Test

Five groups of standard cylindrical carbonate samples were selected for uniaxial compression tests at a loading rate of 0.5 mm/min, with axial and circumferential deformation recorded synchronously to obtain uniaxial compressive strength (UCS), static elastic modulus, and static Poisson's ratio. Here, only the UCS experimental measurement is of concern.

3. Results and Analysis

3.1. Baseline Parameters in the Original State

In the original state (conventional room temperature, unsoaked), the cuttings from the scratch test were in the form of very fine powder, indicating that the consumption of rock internal energy was relatively thorough. The mechanical parameters measured by scratch tests on five core samples are given in Table 3. The overall average UCS is 179.9 MPa, the average internal friction angle is 34.2°, the average cohesion is 47.6 MPa, and the number of effective data points is 4301. The differences between individual samples are obvious: the UCS distribution range is 140.3–203.8 MPa, with the maximum value approximately 1.45 times the minimum; according to equal-weight statistics of the five samples, the arithmetic mean UCS is 181.8 MPa, the standard deviation is approximately 24.9 MPa, and the coefficient of variation is approximately 13.7%, indicating that the grainstone in this reservoir has moderately strong mechanical heterogeneity. The internal friction angle is relatively stable, with a distribution range of 32.1–35.4°, and its dispersion is significantly lower than that of UCS and cohesion, indicating that the friction characteristics between particles of different samples are similar, while differences in cementation degree and load-bearing skeleton are the main source of strength differentiation. The force–displacement curves of the two parallel scratches of each sample followed consistent trends with good repeatability, and this group of data can serve as the baseline for subsequent condition comparison.

Figure 2a presents the scratch force–displacement curve of a typical sample in the original state, and Figure 2b presents the corresponding rock strength parameter calculation result curve. The curve is overall smooth with high-frequency small fluctuations, the latter reflecting the non-uniformity of mineral distribution inside the sample, which is a manifestation of the structural heterogeneity of grainstone and also a manifestation of the discontinuity of the microscopic process of rock fragmentation.

Table 3. Mechanical parameters of each sample in the original state (unsoaked).

Sample No.	Scratch Depth/mm	UCS/MPa	Internal Friction Angle/(°)	Cohesion/MPa	Effective Points
1-4-3	0.25	140.3	32.1	38.8	959
2-7-1	0.25	178.4	34.3	47.3	880
2-7-3	0.25	203.8	35.4	52.7	590
2-8-1	0.25	194.9	35.0	50.9	992
2-8-2	0.25	191.7	34.6	50.4	880
Overall (point-weighted)	—	179.9	34.2	47.6	4301

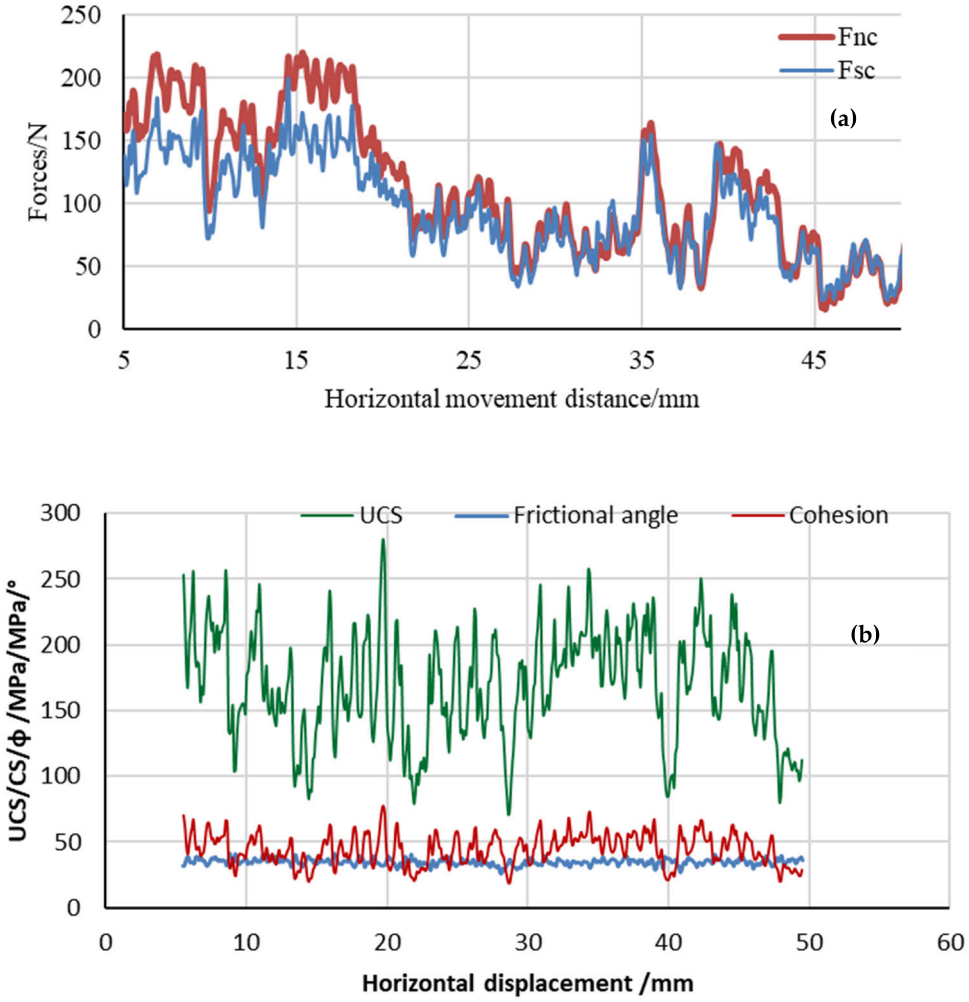


Figure 2. Scratch force–displacement curve and strength parameter result curve of a typical sample (1-4-3, original state). (**a**) Force–displacement curve; (**b**) strength parameter calculation result curve.

3.2. Drilling-Fluid 0 h Instantaneous-Contact Condition

The results of five samples tested immediately after instantaneous wetting by drilling fluid are given in Table 4. The overall average UCS is 191.6 MPa, the internal friction angle is 34.4°, and the cohesion is 50.5 MPa, representing increases of 6.5%, 0.7%, and 6.1%, respectively, relative to the original baseline. The distribution ranges of internal friction angle and cohesion are 33.9–35.5° and 48.3–52.9 MPa, respectively, and the indicators of all samples are at or above the original baseline.

Table 4. Mechanical parameters of each sample under the drilling-fluid 0 h instantaneous-contact condition.

Sample No.	UCS/MPa	Internal Friction Angle/(°)	Cohesion/MPa	Effective Points
1-4-1	195.6	35.5	50.4	1056
1-4-2	188.2	34.2	49.6	976
2-4-1	192.8	34.0	51.5	864
2-5-1	181.1	33.9	48.3	880
2-5-2	199.9	34.4	52.9	848
Overall (point-weighted)	191.6	34.4	50.5	4624

The reason for this phenomenon is that under instantaneous wetting conditions, the drilling fluid does not have time to invade the interior of the sample along pores and microfractures, and cannot fully interact physically and chemically with the intergranular cement, and thus it does not weaken the load-bearing skeleton of the rock; at the same time, the filling of solid particles and liquid phases in the drilling fluid into the surface microfractures of the sample slightly increases the resistance experienced by the cutter during scratching, which manifests as a small increase in apparent strength in the scratch-method inversion. It must be emphasized that this increase is an apparent effect at the testing-method level and should not be taken as evidence that drilling fluid has a substantive "strengthening" effect on the rock; in engineering valuation, it should be understood as "no strength degradation has occurred."

3.3. Fresh Water 24 h Immersion Condition

The results after constant-temperature fresh water immersion for 24 h are given in Table 5. The overall average UCS is 186.0 MPa, the internal friction angle is 33.2°, and the cohesion is 50.2 MPa, representing changes of +3.4%, −2.9%, and +5.4%, respectively, relative to the original baseline. Since this condition uses the same batch of samples as the original condition in Table 3, sample-by-sample comparison is possible: sample 1-4-3 decreased from 140.3 MPa to 137.2 MPa (−2.2%), sample 2-7-1 was essentially unchanged (178.4 MPa vs. 178.3 MPa), and samples 2-7-3, 2-8-1, and 2-8-2 increased from 203.6, 194.9, and 191.7 MPa to 203.9, 201.7, and 213.8 MPa, with changes of +0.1%, +3.5%, and +11.5%.

Table 5. Mechanical parameters of each sample under the fresh water 24 h immersion condition.

Sample No.	UCS/MPa	Internal Friction Angle/(°)	Cohesion/MPa	Effective Points
1-4-3	137.2	30.1	39.5	896
2-7-1	178.3	33.3	48.4	880
2-7-3	203.9	34.7	53.5	590
2-8-1	201.7	34.6	53.1	992
2-8-2	213.8	33.7	57.4	880
Overall (point-weighted)	186.0	33.2	50.2	4238

It can be seen that long-term fresh water immersion did not produce a substantive weakening effect on this grainstone. The mineralogical reason is that grainstone is dominated by carbonate minerals with a low content of water-sensitive components such as clay minerals, so the material basis for hydration swelling and dispersion is weak, and simple formation-water invasion can hardly destroy the intergranular cementation structure. The small decrease in internal friction angle (approximately 1°) and the small increase in cohesion are within the range of testing error and heterogeneity effects and are insufficient to support the judgment that "fresh-water immersion causes strength degradation."

3.4. Drilling-Fluid 24 h Immersion Condition

The results after constant-temperature drilling-fluid immersion for 24 h are given in Table 6. The overall average UCS is 190.9 MPa, the internal friction angle is 33.8°, and the cohesion is 51.0 MPa, representing changes of +6.1%, −1.1%, and +7.0%, respectively, relative to the original baseline. Compared with the drilling-fluid 0 h instantaneous-contact condition, the overall UCS changed from 191.6 MPa to 190.9 MPa, a relative change of only −0.3%, and the cohesion changed from 50.5 MPa to 51.0 MPa, essentially unchanged, indicating that within the range of 0–24 h, the time effect of drilling-fluid action is not significant.

Table 6. Mechanical parameters of each sample under the drilling-fluid 24 h immersion condition.

Sample No.	UCS/MPa	Internal Friction Angle/(°)	Cohesion/MPa	Effective Points
1-4-1	194.2	34.5	51.1	1056
1-4-2	181.5	33.9	48.1	976
2-4-1	199.3	33.3	53.9	864
2-5-1	178.4	33.3	48.2	880
2-5-2	202.2	33.9	54.0	848
Overall (point-weighted)	190.9	33.8	51.0	4624

Sample-by-sample comparison of Tables 4 and 6 likewise supports the above judgment: sample 1-4-1 slightly decreased from 195.6 MPa to 194.2 MPa (−0.7%), sample 1-4-2 decreased from 188.2 MPa to 181.5 MPa (−3.6%), sample 2-4 increased from 192.8 MPa to 199.3 MPa (+3.4%), sample 2-5-1 decreased from 181.1 MPa to 178.4 MPa (−1.5%), and sample 2-5-2 increased from 199.9 MPa to 202.2 MPa (+1.2%). The change directions of the samples are inconsistent and the magnitudes are small, which is the result of the combined action of sample heterogeneity and testing error, rather than systematic strength degradation.

For the tested grainstone samples, no systematic measurable strength degradation was detected within the 24 h water-based-fluid immersion timescale. This does not rule out possible strength alteration under longer-duration, higher temperature-pressure reservoir conditions.

3.5. Acid 24 h Immersion Condition

Figure 3 shows the specimen after 24 h acid immersion. After 24 h of acid immersion, the carbonate specimen exhibits pronounced heterogeneous dissolution. The interfaces between argillaceous-rich laminae and carbonate matrix act as mechanical weak planes, where interlaminar microcracks readily develop and serve as preferential pathways for acid penetration [17,18]. Clay minerals are nearly inert to acid attack, and intensive dissolution takes place within the carbonate matrix once acid arrives, resulting in deeper dissolution pits in the matrix zone. The surface of the scratch test track becomes rough and porous due to the degradation of mineral cementation. As the matrix is dissolved, interlaminar support is lost, triggering the opening of interlayer cracks and partial delamination at the specimen edge. Although the specimen remains intact, the bonding within the rock matrix is substantially weakened. Such uneven damage, governed by preferential acid transport along lamina interfaces and selective matrix dissolution, accounts for the scatter in strength degradation data and justifies the use of a range for the strength calibration factor α.

The results of the scratch test after constant-temperature acid immersion for 24 h are given in Table 7. The overall average UCS decreased to 109.2 MPa, cohesion decreased to 29.0 MPa, and internal friction angle decreased to 27.1°, representing decreases of 39.3%, 39.0%, and 20.6%, respectively, relative to the original baseline, with 4416 effective data points. This is the only condition among the five that exhibits significant strength attenu-

ation, and the attenuation magnitude far exceeds the heterogeneity differences between conditions, with clear physical significance.



Figure 3. The carbonate specimen 2-1-2 after 24 h acid immersion. Interfaces between argillaceous laminae and carbonate matrix provide preferential flow pathways for acid, and intensive dissolution occurs within the carbonate matrix.

Table 7. Mechanical parameters of each sample under the acid 24 h immersion condition.

Sample No.	UCS/MPa	Internal Friction Angle/(°)	Cohesion/MPa	Effective Points
1-1-1	64.5	32.4	17.6	896
1-2-1 (0.18 mm)	84.2	13.7	22.1	800
2-1-2	107.8	20.1	28.3	768
2-3-1	109.7	34.6	28.9	960
2-3-2	170.2	31.6	45.7	992
Overall (point-weighted)	109.2	27.1	29.0	4416

The weakening magnitudes of individual samples differ greatly: the UCS distribution range is 64.5–170.2 MPa, with the highest value 2.64 times the lowest; the cohesion distribution range is 17.6–45.7 MPa; and the internal friction angle distribution range is 13.7–34.6°. Among them, sample 1-2-1 (0.18 mm cutting depth) has an internal friction angle of only 13.7°, which is an abnormally low value related to the extremely non-uniform surface structure after acid dissolution. The force–displacement curves of the two parallel scratches of each sample still highly overlap, indicating reliable experimental repeatability; however, the curve fluctuations are significantly enhanced compared with the original state, directly reflecting the surface unevenness and internal structural damage caused by acid dissolution.

3.6. Comprehensive Comparison of Five Conditions and Degradation Mechanism

The overall strength parameters of the five conditions are summarized in Table 8, with the rates of change all based on the original conventional room-temperature condition. Figures 4 and 5 present the comparison of UCS and cohesion for the five conditions, respectively, and Figure 6 presents the variation trend of UCS with acid immersion time. As can be seen from Table 8 and Figure 4, the UCS values of the three conditions—drilling fluid 0 h, fresh water 24 h, and drilling fluid 24 h—are 191.6, 186.0, and 190.9 MPa, respectively, all not lower than the original baseline of 179.9 MPa listed in Table 3; the differences among the three (approximately 5.5 MPa) are smaller than the heterogeneity span between individual samples and can be considered to be at the same level; whereas the UCS of the acid 24 h

condition drops sharply to 109.2 MPa, clearly deviating from the above range. Cohesion exhibits exactly the same pattern (Figure 5).

Table 8. Summary of overall strength parameters for five working conditions and rates of change relative to the original state.

Working Condition	UCS/MPa	ΔUCS/%	Internal Friction Angle/(°)	Δφ/%	Cohesion/MPa	ΔC/%	Effective Points
As-received (unsoaked) condition	179.9	—	34.2	—	47.6	—	4301
Drilling fluid 0 h	191.6	+6.5	34.4	+0.7	50.5	+6.1	4624
Fresh water 24 h	186.0	+3.4	33.2	−2.9	50.2	+5.4	4238
Drilling fluid 24 h	190.9	+6.1	33.8	−1.1	51.0	+7.0	4624
Acid 24 h	109.2	−39.3	27.1	−20.6	29.0	−39.0	4416

Note: Δ is the rate of change relative to the original conventional room-temperature condition, calculated from the values in the table as (condition value − original value)/original value; each condition value is the overall average after removing 10% from both the beginning and end and weighting by the number of effective points.

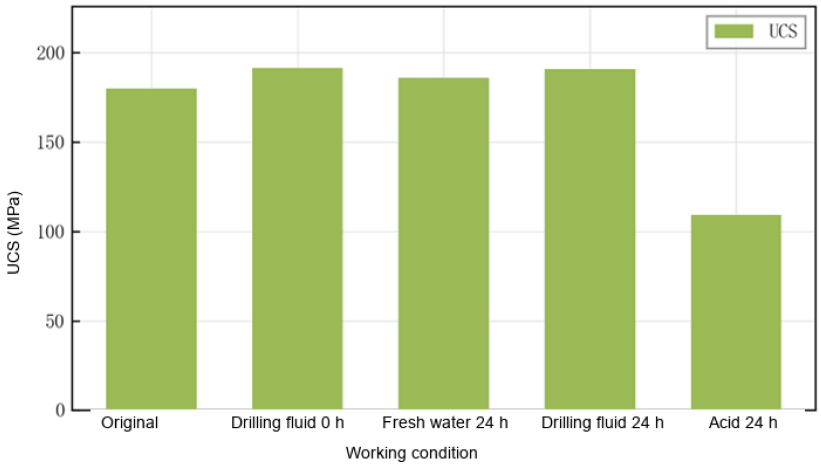


Figure 4. Comparison of overall uniaxial compressive strength (UCS) for five working conditions.

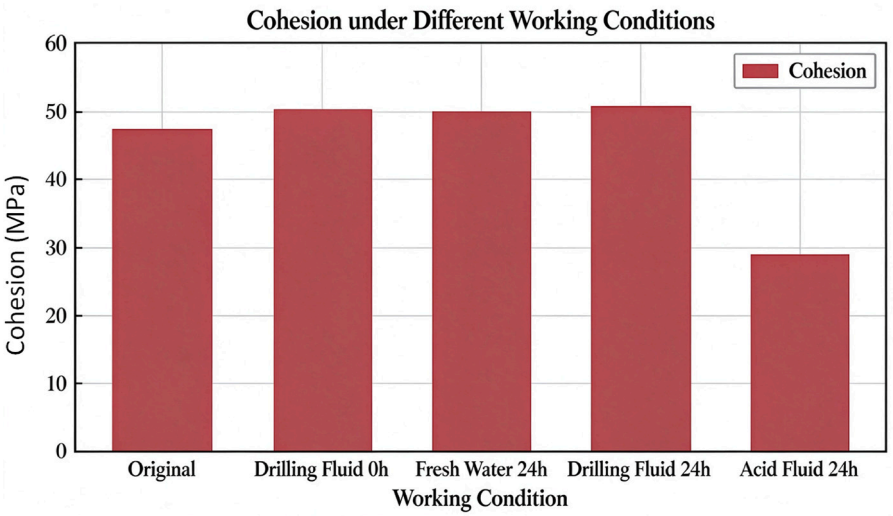


Figure 5. Comparison of overall cohesion for five working conditions.

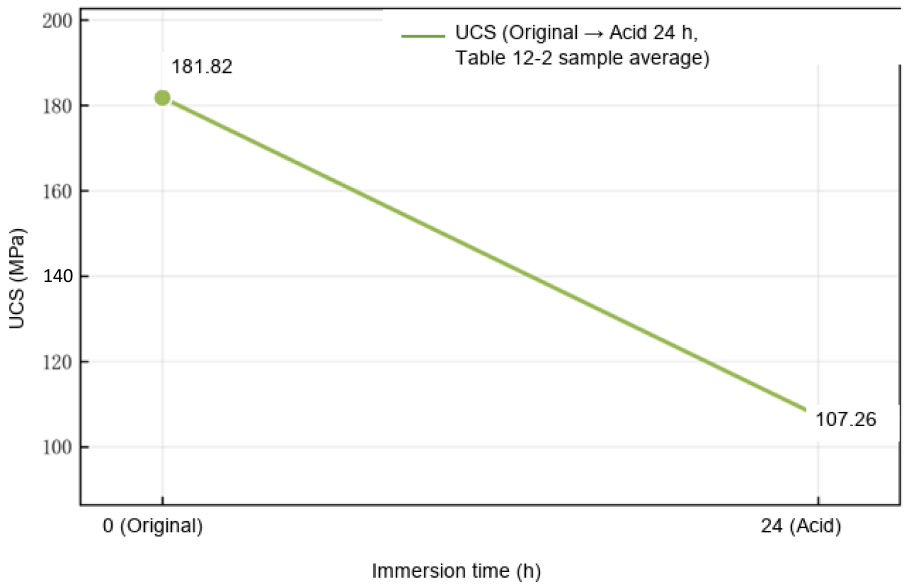


Figure 6. Variation trend of uniaxial compressive strength with immersion time (original → acid 24 h).

To exclude the interference of sample heterogeneity on the conclusions, the paired results of the same batch of control samples (numbered 2-1-1, 2-1-2, 2-3-1, 2-3-2) in the original state and after acid 24 h immersion were further compared, as shown in Table 9. After acid action, the UCS decreased from the equal-weight average of 173.4 MPa to 107.3 MPa, with an average reduction of 38.1%; the cohesion decreased from 46.1 MPa to 28.5 MPa, with an average reduction of 38.1%, highly consistent with the condition-level statistical results (39.3%, 39.0%), verifying the robustness of the strength-attenuation conclusion.

Table 9. Paired comparison of strength parameters before and after acid immersion for the same batch of control samples.

Sample No.	Original UCS/MPa	Post-Acid UCS/MPa	ΔUCS/%	Original C/Mpa	Post-Acid C/MPa	ΔC/%
1-1-1	110.8	64.5	−41.8	29.6	17.6	−40.8
1-1-2 (0.18 mm)	152.0	84.2	−44.6	40.6	22.1	−45.6
2-1-2	198.5	107.8	−45.7	52.1	28.3	−45.7
2-3-1	210.8	109.7	−48.0	56.3	28.9	−48.6
2-3-2	194.8	170.2	−12.6	51.6	45.7	−11.5
Equal-weight average	173.4	107.3	−38.1	46.1	28.5	−38.1

Note: The original values are the arithmetic means of the two parallel scratches of that sample; the post-acid values are taken from the same-numbered sample in the acid 24 h immersion condition.

At the same time, it can be seen that the reduction magnitudes of the samples differ significantly: the UCS reductions in samples 1-1-1, 1-1-2 (0.18 mm), 2-1-2, and 2-3-1 are between 41.8% and 48.0%, while sample 2-3-2 with higher initial strength has a reduction of only 12.6%. This indicates that the magnitude of acid weakening depends on the mineral composition, pore structure, and cementation type of the sample itself: samples with high cement content and good pore connectivity are more susceptible to acid dissolution along pores and cementation interfaces, resulting in more severe strength attenuation. Cement dissolution inference is derived from macroscopic mechanical changes only. Quantification of acid penetration depth, micro imaging, and mineral chemical tests are proposed as critical future work tasks.

Mechanistically, acid promotes dissolution reactions with carbonate minerals, preferentially dissolving intergranular cement and enlarging pores and dissolution vugs, causing the rock to degenerate from a densely cemented load-bearing skeleton to a loose structure with weakened intergranular connections. This mechanism manifests in parameter changes as cohesion and UCS decrease synchronously and substantially (reduction of approximately 39%), while the decrease in internal friction angle is relatively small (20.6%). Since the internal friction angle mainly reflects the friction characteristics and interlocking action of particle surfaces, while cohesion directly reflects cementation strength, the above "cohesion-dominated" attenuation characteristic indicates that strength degradation is dominated by cementation-structure destruction rather than changes in intergranular friction characteristics. This understanding is consistent with existing research conclusions that acidification leads to decreased strength and stiffness of carbonate rocks and transformation of mechanical behavior from brittle to ductile [14,15]. Therefore, in engineering evaluation, UCS and cohesion should be prioritized when judging rock integrity, rather than drawing conclusions solely from changes in internal friction angle.

Conversely, water-based drilling fluid and fresh water did not cause strength decline within the 24 h scale, because grainstone has a low content of water-sensitive minerals, hydration lacks a material basis, and the filtrate can hardly effectively invade the dense limestone matrix in a short time. Thus, it can be clarified that for this batch of ultra-deep carbonate rocks, water-based working fluids are not the dominant factor of strength degradation, while acid action is the controlling factor; the two belong to different working conditions and should not be confused in engineering design and parameter valuation.

3.7. Influence of Scratch Depth and Sample Heterogeneity

Scratch depth is the most critical controllable variable in scratch testing. Tests were conducted on the same sample 1-1-2 using cutting depths of 0.18 mm and 0.20 mm, respectively, and the results are shown in Table 10. At 0.18 mm cutting depth, the UCS, internal friction angle, and cohesion are 152.0 MPa, 33.6°, and 40.6 MPa, respectively; at 0.20 mm cutting depth, they decrease to 105.9 MPa, 30.4°, and 28.4 MPa, with reductions of 30.3%, 9.6%, and 30.1%.

Table 10. Influence of scratch depth on mechanical parameter test results (from sample 1-1-2).

Scratch Depth/mm	Scratch No.	UCS/MPa	Internal Friction Angle/(°)	Cohesion/MPa
0.18	Scratch 1	141.4	33.9	37.6
0.18	Scratch 2	162.6	33.2	43.7
0.18	Average	152.0	33.6	40.6
0.20	Scratch 1	96.6	28.6	25.9
0.20	Scratch 2	115.1	32.1	31.0
0.20	Average	105.9	30.4	28.4

The mechanical reason is that with increasing cutting depth, rock cutting gradually transitions from the ductile mode to the brittle mode; in the brittle mode, crack propagation and cutting spalling reduce the energy per unit volume of fragmentation, the average resistance experienced by the cutter decreases, and the inverted apparent strength decreases accordingly [8,10]. This indicates that what the scratch method measures is apparent strength bound to the test conditions, and only under unified cutting depth and unified test rate can data between different samples and different conditions be horizontally comparable. The main experiments in this paper uniformly adopted the standard cutting depth of 0.25 mm precisely for this reason, while sample 1-1-2 in the acid group adopted a cutting depth of 0.18 mm, and this difference should be noted when comparing with other samples in the same group.

Sample heterogeneity is likewise a non-negligible influencing factor. Taking the six samples of the control batch in the original state as an example, the UCS distribution range is 105.9–210.8 MPa, with a range close to 100 MPa; even under the same working conditions and the same test conditions, there may still be multiple-fold differences between different samples. This heterogeneity originates from spatial differences in mineral composition, particle size, and cementation degree formed during the sedimentation and diagenesis of grainstone. Therefore, field drilling and stimulation design should not adopt unified construction parameters, but should be designed differentially by layer and interval; laboratory experiments should ensure a sufficient number of parallel samples and use the statistical mean of multiple samples as the representative value of the working conditions.

3.8. Calibration of Strength Calibration Factor α

A rigid testing machine was used to perform conventional UCS measurement on rock specimens. The measured UCS results are listed in Table 11. Table 11 also lists the measured values of elastic modulus and Poisson's ratio of these specimens, the purpose of which is to show that the material composition of the rock differs between samples, which may be a factor leading to different UCS values. Table 11 also lists the average of the UCS results obtained by scratch tests on conventional original-state specimens.

Table 11. Uniaxial compressive strength test and calibration of strength calibration factor α.

Sample No.	Test Type	UCS/MPa	Elastic Modulus/GPa	UCS Average/MPa	Scratch-Test UCS/MPa (from Table 3)	Strength Calibration Factor α
2-1-1	Uniaxial mechanical property test	82.3	23.5	84.7	179.9	0.47
2-1-3	Uniaxial mechanical property test	87.1	23.9			
2-2-2	Uniaxial mechanical property test	110.1	34.1	109.9		0.61
2-6-2	Uniaxial mechanical property test	106.5	32.6			
2-7-2	Uniaxial mechanical property test	113.1	37.3			

As shown in Table 11, the five tested samples were divided into two groups for averaging based on their measured uniaxial compressive strength (UCS). The average UCS of the two groups is 84.7 MPa and 109.9 MPa, respectively. These values are markedly lower than the overall average UCS (179.9 MPa), which was derived from the intrinsic specific energy of the corresponding samples using the scratch test method. The corresponding strength calibration factors are 0.47 and 0.61, respectively. Given the heterogeneity of the carbonate rock samples, the strength calibration factor α may be taken as 0.47–0.61.

In practice, uniaxial compression uses standard cylindrical specimens containing natural fractures and micropores. The UCS given by the rigid testing machine is the strength in the sense of overall failure. The UCS value given by the scratch method reflects the cutting resistance of the near-surface shallow layer of the sample locally at a given cutting depth, and its absolute value is affected by cutting depth, cutter state, and the conversion relationship. The UCS value obtained by rigid-testing-machine uniaxial compression is the UCS value used in the conventional sense for wellbore stability analysis. Therefore, the UCS data given by the scratch method need to be calibrated by the strength calibration factor α before they can be used in engineering applications.

4. Engineering Application Discussion

Based on the above experimental results, further condition-specific strength parameters that can be directly cited for ultra-deep carbonate wellbore stability analysis and multi-field-coupled calculation are given in Table 12. In the table, only UCS is converted in combination

with the strength calibration factor. Here, the value of the strength calibration factor is set as $\alpha = 0.56$, which is in the range of 0.47~0.61. The magnitude of the friction angle is not converted, because the value of the friction angle is related to rock particle size and relatively less related to cementation degree. The cohesion value is also converted as a result of the UCS conversion. The converted UCS values of acid-immersed samples presented in Table 12 serve as preliminary engineering references for a selected α, which incorporates the practical experience of field engineers.

Table 12. Recommended values of strength parameters for collapse-pressure and multi-field-coupled calculations.

Working Condition	Scratch-Method UCS/MPa	Internal Friction Angle/(°)	UCS Converted with α	Cohesion/MPa
As-received (unsoaked) condition	179.9	34.2	100.7	26.7
Drilling fluid 0 h instantaneous contact	191.6	34.4	107.3	28.3
Fresh water 24 h immersion	186.0	33.2	104.2	28.2
Drilling fluid 24 h immersion	190.9	33.8	106.9	28.5
Acid 24 h immersion	109.2	27.1	61.2	18.7

In collapse-pressure calculation and safe mud-weight window design, the drilling-fluid and fresh water conditions can be valued according to the corresponding measured values in Table 12. Among them, the acid condition must be handled as a separate case, using the weakened UCS, internal friction angle, and cohesion as inputs, and evaluated together with the field acid concentration, action time, and reservoir-stimulation fluid configuration system.

It should also be noted that the condition of this experiment is that the acid condition adopts simplified constant-temperature acid immersion for 24 h, which does not reproduce the complete field process of "pad-fluid fracture creation—acid—corrosion inhibitor—multi-fluid alternating injection," nor does it consider the effects of temperature, confining pressure, and fluid-flow shear.

5. Conclusions

This study presents a systematic experimental investigation of rock strength parameters for ultra-deep carbonate reservoirs (>9000 m) under multiple working conditions, combining continuous scratch testing with conventional uniaxial compression. The main conclusions are as follows:

(1). Continuous scratch testing provides a reliable, minimally destructive approach for obtaining strength profiles of ultra-deep carbonate rocks. For grainstone from the YS Section of Well XY in its original state, the scratch-test-derived UCS, internal friction angle, and cohesion are systematically higher than those obtained from rigid-testing-machine uniaxial compression. A ratio coefficient $\alpha = 0.56$ is calibrated to convert scratch-method UCS to engineering-recommended values, yielding a baseline UCS of approximately 100.7 MPa for collapse-pressure and multi-field-coupled calculations.

(2). Water-based working fluids—including field drilling fluid and fresh water—do not cause measurable strength degradation of grainstone within a 24 h time scale under room temperature. Both instantaneous contact and prolonged immersion maintain or slightly increase the measured UCS and cohesion, attributable to the low clay-mineral content and weak water sensitivity of the carbonate matrix. This finding suggests that, for lithologies similar to the studied grainstone, short-term water-based fluid invasion during drilling is unlikely to be a dominant wellbore-stability risk factor.

(3). Acid immersion is the only condition among the five tested that produces significant strength attenuation. After 24 h exposure to 15% hydrochloric acid, the scratch-method UCS and cohesion decrease by approximately 39%, and the internal friction angle decreases by approximately 21%. The weakening is driven primarily by the dissolution of intergranular cement and the associated enlargement of pores and dissolution vugs, which transforms the rock from a dense, continuous medium toward a porous, fragmented one.

(4). The magnitude of acid-induced weakening exhibits strong sample dependence, with individual UCS reductions ranging from approximately 13% to 48%. This variability reflects differences in initial mineral composition, pore structure, and cementation quality among samples, and implies that a single acid-weakening factor may be insufficient for field design—site-specific characterization is advisable.

(5). Scratch depth is a critical controllable variable that must be standardized in comparative experiments. Increasing the cutting depth from 0.18 mm to 0.20 mm reduces the measured UCS by approximately 30%, as the cutting mechanism transitions from a ductile-dominated to a brittle-dominated regime. The acid-condition tests in this study employed variable scratch depths (0.18–0.25 mm), which may contribute to the observed scatter and should be unified in future work.

Limitations and future work. This study is subject to several constraints: (i) all experiments were conducted at room temperature and atmospheric pressure, whereas the target reservoir experiences high temperature and high confining pressure at >9000 m depth; (ii) the acid immersion used a simplified constant-temperature, constant-concentration protocol that does not replicate the dynamic acid-fracturing process in the field; (iii) the ratio coefficient α was calibrated using only five original-state samples and has not been independently validated for acid-weakened rock. (iv) No plug-resolved petrography, SEM/CT or porosity data were acquired for the scratch-tested cores. Microstructural characterization before and after fluid exposure should be carried out in follow-up studies to physically verify the cement dissolution mechanism. (v) Future work should integrate petrographic observation, XRD mineral quantification, and porosity measurements for each tested plug to link mechanical evolution to rock fabric and mineral composition. Future studies should address these gaps by conducting temperature- and pressure-controlled experiments, dynamic acid-rock reaction tests under flowing conditions, and microstructural characterization (e.g., SEM, CT scanning, porosity measurement) before and after fluid exposure to substantiate the degradation mechanisms. The dataset and calibrated α coefficient presented herein can serve as a preliminary reference for wellbore stability evaluation and acid-fracturing parameter optimization in ultra-deep carbonate reservoirs.

Author Contributions: Conceptualization, Z.L. and X.S.; methodology, Z.L., X.S. and W.M.; software, Y.S.; validation, Z.L., G.S. and J.L.; formal analysis, Z.L.; investigation, Z.L. and W.M.; resources, W.M. and G.S.; data curation, Y.S. and J.L.; writing—original draft preparation, Z.L.; writing—review and editing, X.S.; visualization, Y.S.; supervision, X.S.; project administration, W.M.; funding acquisition, X.S. All authors have read and agreed to the published version of the manuscript.

Funding: This research was funded by the Talent Fund Project of Liaoning Petrochemical University (Grant No. 1100130301) and the National Natural Science Foundation of China (Grant No. 52574041).

Institutional Review Board Statement: Not available.

Informed Consent Statement: Not available.

Data Availability Statement: The data presented in this study are available on request from the corresponding author. The data are not publicly available due to confidentiality restrictions related to the field data.

Conflicts of Interest: The authors declare no conflicts of interest.

Abbreviations

The following abbreviations are used in this manuscript:

UCS	Uniaxial Compressive Strength
ECD	Equivalent Circulating Density
LVDT	Linear Variable Differential Transformer
DD model	Detournay–Defourny model

References

1. *ASTM D7012-10*; Standard Test Method for Compressive Strength and Elastic Moduli of Intact Rock Core Specimens Under Varying States of Stress and Temperatures. ASTM International: West Conshohocken, PA, USA, 2010.
2. Ulusay, R.; Hudson, J.A. (Eds.) *The Complete ISRM Suggested Methods for Rock Characterization, Testing and Monitoring: 1974–2006*; ISRM: Ankara, Turkey, 2007.
3. Bieniawski, Z.T. The effect of specimen size on compressive strength of coal. *Int. J. Rock Mech. Min. Sci.* **1968**, *5*, 325–335. [CrossRef]
4. Chau, K.T.; Wong, R.H.C. Uniaxial compressive strength and point load strength of rocks. *Int. J. Rock Mech. Min. Sci. Geomech. Abstr.* **1996**, *33*, 183–188. [CrossRef]
5. Detournay, E.; Drescher, A.; Hultman, D.A. Portable Rock Strength Evaluation Device. U.S. Patent 5670711, 23 September 1997.
6. Detournay, E.; Defourny, P. A phenomenological model for the drilling action of drag bits. *Int. J. Rock Mech. Min. Sci. Geomech. Abstr.* **1992**, *29*, 13–23. [CrossRef]
7. Adachi, J.I.; Detournay, E.; Drescher, A. Determination of rock strength parameters from cutting tests. In *Rock Mechanics*; Aubertin, M., Hassani, F.P., Mitri, H., Eds.; Balkema: Rotterdam, The Netherlands, 1996; pp. 1517–1524.
8. Richard, T.; Detournay, E.; Drescher, A.; Nicodème, P.; Fourmaintraux, D. The scratch test as a means to measure strength of sedimentary rocks. In Proceedings of the SPE/ISRM Rock Mechanics Conference, Trondheim, Norway, 8–10 October 1998.
9. Schei, G.; Fjær, E.; Detournay, E.; Kenter, C.J.; Fuh, G.F.; Zausa, F. The scratch test: An attractive technique for determining strength and elastic properties of sedimentary rocks. In Proceedings of the SPE Annual Technical Conference and Exhibition, Dallas, TX, USA, 1–4 October 2000.
10. Richard, T.; Dagrain, F.; Poyol, E.; Detournay, E. Rock strength determination from scratch tests. *Eng. Geol.* **2012**, *147–148*, 91–100. [CrossRef]
11. Liu, H.; Bo, K.; Jin, Y.; Lu, Y.; Zhu, J.; Zhang, Z.; Zhang, F. Method for determining rock strength parameters of complex formations based on continuous scratch experiments. *Pet. Sci. Bull.* **2022**, *7*, 532–542. (In Chinese)
12. Chen, S.; Hu, D.; Zhou, H. Research on continuous dynamic core scratching test technology. *ChinaXiv* **2025**, ChinaXiv:202507.00370. (In Chinese)
13. Zhao, Y.; Wang, T.; Yang, Z.; Xie, R. Classification criterion for coal burst propensity based on scratch testing. *Coal Sci. Technol.* **2025**, *53*, 117–127. (In Chinese)
14. Abdulraheem, A. Impact of HCl acidizing treatment on mechanical integrity of carbonaceous shale. *ACS Omega* **2022**, *7*, 13629–13643. [CrossRef] [PubMed]
15. dos Santos, Y.R.P.; Gomes, I.F.; Lima, A.; Peixoto de Oliveira, G.C. Matrix acidizing impact on the geomechanical properties in carbonate rocks: An experimental approach using acetic acid at different contact times. *Mech. Time-Depend. Mater.* **2025**, *29*, 97. [CrossRef]
16. *SY/T 5367—2019*; Test Method for Uniaxial Compressive Strength of Rock. National Energy Administration of China: Beijing, China, 2019. (In Chinese)
17. Noiriel, C.; Gouze, P.; Bernard, D. Impact of coating development on the hydraulic and transport properties in argillaceous limestone fracture. *Water Resour. Res.* **2007**, *43*, W09406. [CrossRef]
18. Larsen, B.; Gudmundsson, A. Linking of fractures in layered rocks: Implications for permeability. *Tectonophysics* **2010**, *492*, 108–120. [CrossRef]

Disclaimer/Publisher's Note: The statements, opinions and data contained in all publications are solely those of the individual author(s) and contributor(s) and not of MDPI and/or the editor(s). MDPI and/or the editor(s) disclaim responsibility for any injury to people or property resulting from any ideas, methods, instructions or products referred to in the content.